IEEE Access
Multidisciplinary | Rapid Review | Open Access Journal

Received April 15, 2020, accepted May 4, 2020, date of publication May 7, 2020, date of current version May 21, 2020.

Digital Object Identifier 10.1109/ACCESS.2020.2993178

Adaptive and Fuzzy PI Controllers Design for Frequency Regulation of Isolated Microgrid Integrated With Electric Vehicles

MISHKAT ULLAH JAN[1], AI XIN[1], MOHAMED ABDELKARIM ABDELBAKY[1,2], HASEEB UR REHMAN[1], AND SHEERAZ IQBAL[1,3]

[1]State Key Laboratory of Alternate Electrical Power System with Renewable Energy Source, North China Electric Power University, Beijing 102206, China
[2]Department of Electrical Power and Machines, Faculty of Engineering, Cairo University, Giza 12613, Egypt
[3]Department of Electrical Engineering, University of Azad Jammu and Kashmir, Muzaffarabad 13100, Pakistan

Corresponding authors: Mishkat Ullah Jan (engrmishkat@ncepu.edu.cn) and Mohamed Abdelkarim Abdelbaky (m_abdelbaky@ncepu.edu.cn)

This work was supported in part by the Beijing Natural Science Foundation under Grant 3182037, and in part by the Fundamental Research Funds for the Central Universities under Grant 2019QN041.

ABSTRACT The number of electric vehicles and renewable energy resources integrated into the power system is increasing day by day. The objective behind the development of electric vehicles and renewable energy sources is to build a sustainable and green power system. The renewables either don't possess system inertia or have less system inertia, therefore, they don't effectively respond to the load variations. The battery storage system of electric vehicles is used as the first line of defense to counter the effect of load/frequency variations and make the system stable. As active power is inversely proportional to the system frequency, for this purpose electric vehicles are included in the microgrid environment. In this paper, an isolated microgrid having a reheat turbine system, wind turbine system, photovoltaic system, and electric vehicles is studied. The output of the renewables is not controlled to utilize its maximum output power. Therefore, adaptive droop control and fuzzy PI control mechanisms are implemented to cater to the frequency variations of the isolated microgrid; the former regulates the power of electric vehicles while maintaining the energy needs of each EV and the later controls the output power of reheat turbine system according to the frequency variation. Furthermore, the genetic algorithm optimization toolbox is utilized to optimize the parameters of the adaptive and fuzzy PI controllers. The proposed model is developed in MATLAB/Simulink which shows that these control techniques effectively sustained the system frequency of isolated microgrid in the desired limits.

INDEX TERMS Adaptive droop control, electric vehicles, frequency regulation, fuzzy PI control, GA optimization technique, renewable energy sources, reheat turbine system.

I. INTRODUCTION

Power is the major challenge among all the challenges faced by the world today. Continuous depletion of fossil fuel, growing energy demand, and the rise in pollution converge the world's attention to regulate power usage and diversify its production process. The resolution of the power crisis can help to eradicate poverty and to improve infrastructure development. The proliferation of renewable energy sources (RESs) and the introduction of controllable loads have given rise to the idea of microgrid (MG) [1]. RESs are considered an excellent alternative of conventional energy sources, however, their increasing integration into the power grid caused concerns over system stability [2], [3]. Hence, special considerations are required in management, control, monitoring, and design for these RESs integration into the power system [4].

In conventional power systems, a synchronous generator is used for generating systems nominal voltage and frequency. System stability is achieved with the help of active and reactive power, voltage compensation devices, and droop control. The researchers defined two operational modes of microgrid, which are: (1) grid-connected and (2) isolated mode [5]. The prior mode is supported by the grid to overcome the load variations. Consequently, in the latter mode, it is mandatory to utilize advance, flexible and intelligent control techniques

The associate editor coordinating the review of this manuscript and approving it for publication was Xiaojie Su.

to achieve better stabilization of isolated MG and to provide robust performance in the presence of highly intermittent RESs, having low system inertia and unpredictable load variations [6]. Therefore, the energy storage system (ESS) is included in the MG to sustain the system frequency deviation at a minimal value [7].

To counter the effect of the aforementioned challenges various energy storage technologies are implemented to overcome the power mismatch between the generation and consumption, and the frequency fluctuations in MG [8]. The approach of ESS was firstly introduced in New York City in the late 19th century to energize the street lamps at night to turn off the generators [9]. ESS is presently the essential component in the MG as it's a smart way to overwhelm the probable power imbalance challenges and purposes as a backup reservoir or buffer zone to respond immediately under load variation conditions [10]. As the emergence of electric vehicles (EVs) in the recent era developed the vehicle to grid (V2G) concept, where the EVs batteries are utilized to abridge the generation shortfall when the RESs are not operating at their expected output [11]. Therefore, EVs are considered mobile ESS which possesses the ability to provide ancillary services to MG. Hence, the EVs' role in the participation of MG frequency control is more vital and evident.

Droop control techniques and their advanced versions are widely used for frequency regulation of the power system due to the absence of communication links [12]. The droop control mechanism in synchronous generators is used to regulate the output power according to the load variations in allowable limits in multiple microgrids [13]. In the meantime, the ESS approach is developed which mimics the droop characteristic of the synchronous generator to counter the effect of power fluctuation and provide frequency support to isolated MG [14]. The authors propose an adaptive fuzzy droop control technique for the optimization of active power-sharing in an isolated MG by adjusting the power frequency droop coefficients. A secondary control mechanism is considered to stabilize the frequency and voltage [14]. The recent development in the control mechanisms to regulate the aerodynamics and resilient control of EVs are studied by various researchers [15], [16].

Due to the charging and discharging power capabilities of the EVs, their introduction makes the structure of MG more interesting to regulate the frequency deviation [17]. A single EV has very little impact on providing ancillary services to MG, therefore a bulk of EVs are considered in [18] to provide peak load shifting [19], spinning reserve [20], voltage regulation [21] and most importantly frequency regulation. The adaptive droop control technique is used in [22] for the regulation of the frequency of a multi-area system integrated with EVs. There are certain limitations of droop controllers such as poor transient performance, inability to provide accurate power-sharing with output considering impedance uncertainties, in-appropriateness for nonlinear loads, and incapability to enact a fixed system frequency when used in multi-resources MG [23]. Therefore, a combination of controllers can effectively regulate the isolated MG frequency deviation.

The frequency regulation aims to reduce the frequency deviation by changing the active power of certain units either by increasing or by decreasing the power generation of the distributed generators [24]. The random variations in the load demand affect the frequency of the distributed generators of the power system [25]. The hydro storage unit is added to rescue the RTS when there occurred a load mismatch (frequency variation) [26]. Meanwhile, the control systems are now becoming a vital component in the electrical networks [27], due to their easy implementation. Mostly the researchers are keen to practice conventional controllers such as proportional Integral (PI) [28] or proportional Integral-derivative (PID) [29] for power system load frequency control. The PI/PID controller proposes good systems performance but it is still not optimal [30]. Besides this, the PID controller based on the Hammerstein type neural network is utilized to regulate the LFC of the multi-area power system [10]. Additionally, the fuzzy logic controller [31], distributed model predictive control [32], and hierarchical distributed model predictive control [33] are also implemented to investigate the frequency regulation in MG. Various optimization methods like a genetic algorithm (GA), jay algorithm, and particle swarm optimization (PSO) are used to optimize the conventional controllers PI/PID and fuzzy PI/PID controller. Meanwhile, their impact is also studied for stabilizing and guarantee their robustness of the load frequency control [34]. However, the above authors didn't consider either one or more parameters, for instance in [31]–[34], the EVs participation is not studied, in [34] RTS is not considered, and in [32] only WTS are investigated. Furthermore, the above-mentioned controllers PI/PID controller's approach has good frequency performances, but their performances are still not optimum, and their parameters were not well-tuned.

The main emphasis of this research is to study the effect of various control schemes on an isolated MG to regulate the system frequency. The following are the key contributions of this paper.

1) RTS, WTS, PV, and EVs are taken into account for potentially active power injectors to regulate the frequency for a multistep and random variable load disturbance and variable conditions of the RESs.
2) Adaptive droop control (ADC) and fuzzy PI control mechanisms are implemented on EVs and RTS, respectively. The ADC technique is implemented on EVs battery to participate effectively in frequency control but primarily it regulates the EVs batteries to be charged to their desired level to fulfill the owner's driving demand.
3) An advanced genetic algorithm toolbox is used to optimize the parameters of ADC and fuzzy PI controllers.

The paper is divided into four sections, in section II the detailed model of an isolated MG is presented, section III provides the details of the ADC, fuzzy PI and advanced

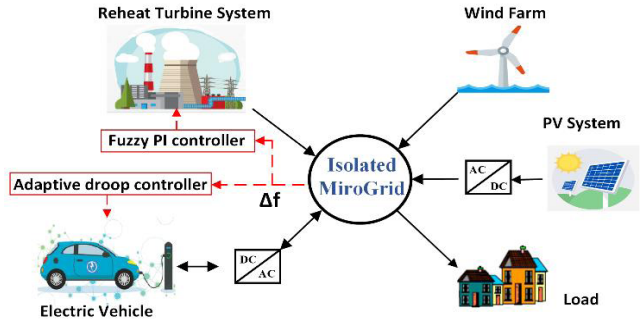

FIGURE 1. The dynamic model of the isolated microgrid.

genetic algorithm optimization toolbox, section IV provides the simulation results and discussions.

II. MODELING OF ISOLATED MICRO-GRID

Various kinds of microgrid's (MG) dynamic model is presented by researchers to assess the frequency regulation in the MG [13], [14], [23]. To evaluate the frequency regulation of isolated MG integrated with RESs and EVs the system equation is given below:

$$\Delta P_{RTS} + \Delta P_{wind} + \Delta P_{PV} \pm \Delta P_{EV} - \Delta P_L = (M.s + D)\,\Delta f \tag{1}$$

Here, M is the system inertia, D is the damping factor and Δf is the system frequency deviation, while ΔP_{RTS}, ΔP_{wind}, ΔP_{PV}, ΔP_{EV}, and ΔP_L are the change in power of reheat turbine system, wind turbine, photovoltaic, EVs, and in load power, respectively. Fig. 1 depicts the overall model of isolated MG and the relevant components. The EVs feed and absorb a sufficient amount of power for a small-time period to keep the system stable. The charging of EVs needs a proper amount of time, so to limit the storage, several second-time constants are considered for frequency control design. In the following section, this work presents the EVs dynamic models in a new way which is based on the latest models. Moreover, the reheat turbine system (RTS) model is introduced to provide active power generation quickly and finally, for the comprehensive cooperation of wind turbine system (WTS) in the frequency control scheme, one dynamic model is presented in a de-loaded area that has sufficient headroom to participate in frequency regulation scheme effectively.

A. MODEL OF THE REHEAT TURBINE SYSTEM

The RTS plays a vital role in power generation since its invention. Though, a variety of steam turbines are vastly implemented in the power system due to their instant, durable, and efficient power production characteristics. Furthermore, the RTS is preferred over the non-reheated turbine because it provides the same amount of electrical power for less fuel. The reheater increases the efficiency ranges between 7 to 8% to convert more of the energy being used to create the steam into the actual output from the turbine. The material

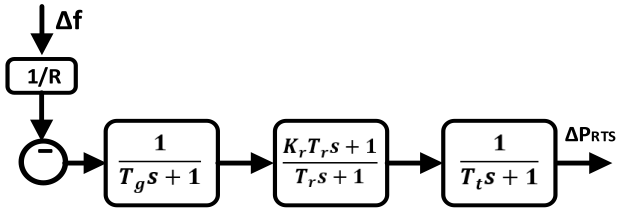

FIGURE 2. The first order of the RST.

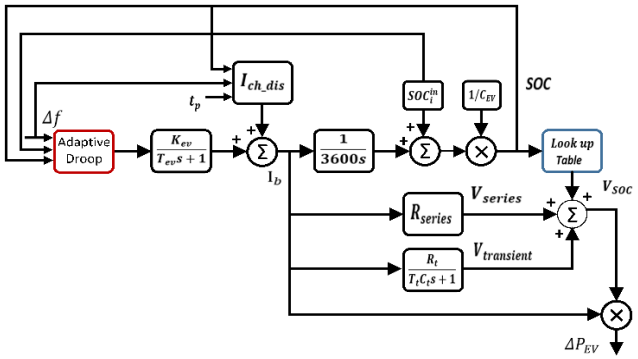

FIGURE 3. The dynamic model of EV [35].

degrading and other properties associated with the RTS model are not considered in this research work.

RTS can adjust its resultant power according to the load demand variations. The first-order transfer function of the RTS model is shown in Fig. 2, where T_g, T_r, and T_t are the governor, reheater, and turbine time constants, respectively. While K_r is reheater gain of the RTS system, which effectively participates in frequency control of MG. Moreover, Δf depicts the frequency fluctuation, and R represents the speed regulation co-efficient of RTS.

B. THE ELECTRIC VEHICLE MODEL

This research work focuses on EVs support in the MG frequency regulation. The internal power loss and type of battery technology are not taken into account. These assumptions don't affect the objectives of this study. The researchers developed several aggregated models of the EV battery to study the MG frequency regulation [22]. In [19], the authors developed a Thevenin equivalent circuit of the EV's battery as shown in Fig. 3. Here, the series voltage (V_{series}) and transient voltage ($V_{transient}$) have a negligible impact on the battery voltage, therefore, the open-circuit voltage (V_{soc}) is solely responsible to be considered while calculating the output power of the EV. Subsequently, the battery is charged and discharged by I_{ch-dis} current. The first order EV transfer function which is widely used in literature is given in (2):

$$P_{EV} = \frac{K_{ev}}{T_{ev}s + 1} \tag{2}$$

where K_{ev} and T_{ev} are the gain and time constant of the EV battery, respectively and C_{EV} *is the* rated capacity of the

battery. The detailed explanation of this model is given in section III.

C. MODEL OF THE WIND TURBINE

The resultant power of wind turbines is considered as a variable natural power resource that is dependent on the wind profile, which varies from time to time. Subsequently, the generic model of the WTS is designed as a power variant entity in an isolated MG. The output power (P_{wind}) and mechanical power (P_{mech}) of WTS are calculated by (3) and (4) [36], [37]:

$$P_{wind} = \eta P_{mech} \tag{3}$$

$$P_{mech} = \frac{1}{2} C_p(\lambda, \beta) A \rho_a V^3 \tag{4}$$

where η and ρ are the WTS's efficiency and air density, respectively; $\lambda = \omega_r R/\upsilon$ is tip speed ratio;ω_r is the angular velocity of the rotor and R is the blade length. As a natural resource, the resultant power of a wind turbine is fluctuating due to the time-variant wind direction and the wind speed (V).

As previously restated in a number of references, the WTS resultant power is defined as a combination of power coefficient C_p and other physical components. Generally speaking, C_p is a function of two fundamental parts including tip speed ratio (λ) and the blade pitch angle (β), it is the power capturing efficiency of the WTS and defined below [39]:

$$C_p = 0.5176\left(\frac{116}{\lambda_i} - 0.4\beta - 5\right)e^{\frac{-21}{\lambda_i}} + 0.0068\lambda \tag{5}$$

where λ_i satisfies the following equation:

$$\frac{1}{\lambda_i} = \frac{1}{\lambda + 0.08\beta} - \frac{0.035}{\beta^3 + 1} \tag{6}$$

The intrinsic features of the wind turbines have minimum influence on the frequency of MG, as far as the distributed generator and EV's controller's performance is intended. Therefore, wind power is clarified as a power variation resource of the isolated MG.

D. MODEL OF PHOTOVOLTAIC SYSTEM

The solar PV system is the first choice for selecting among the RESs, due to the abundance of solar irradiance and easy installation. Solar irradiance and temperature are important parameters while calculating the resultant power of the PV system. The PV resultant power can be calculated in the following equation:

$$P_{PV} = \varphi.S.\xi.(1 - 0.005(T_A - 25)) \tag{7}$$

Here, the conversion efficiency of the PV array is defined by φ, this parameter generally changes from 9% to 12%. S is an effective region of photovoltaic panels in m^2 and ξ is a sign of solar irradiance, which is chosen as 1 kW/m^2. Besides, T_A is an ambient temperature calculated in degree Celsius and is standard operational value is 25 °C. As a consequence, the value of P_{PV} is reliant on the solar irradiance since the parameters S and ξ are constants [40].

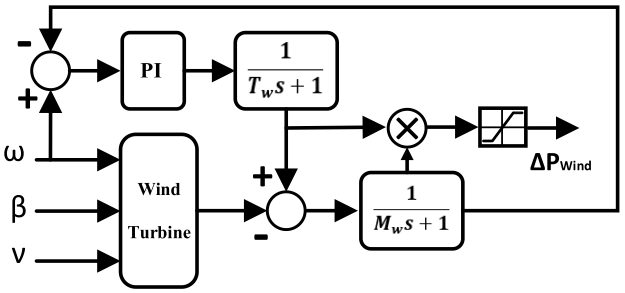

FIGURE 4. The dynamic model of the wind turbine [38].

III. THE PROPOSED CONTROL STRATEGY

A. THE PROBLEM FORMULATION

The prime goal of a microgrid is to maximize the utilization of renewable energy resources and less dependency on fossil fuel plants for a clean and green environment. The typical microgrid (MG) contains different kinds of power generators, loads, controllers, and energy storage systems [4]. As discussed earlier, the isolated MG is more prone to system instabilities like frequency and voltage. In this paper, the reheat turbine system (RTS) and renewable energy sources (RESs) are integrated to make an isolated microgrid. Moreover, electric vehicles (EVs) are used as energy storage units instead of installing separate energy storage units [41], [42]. The main difficulties in the isolated microgrid are to regulate the outpower power of the generators according to the system requirements. Furthermore, the designing of suitable controllers to control the output power of the RTS and regulates the charging and discharging of EVs are important in order to regulate the system frequency. The motivation behind the proposed scheme is to connect both fuzzy PI and adaptive droop controllers in an effective and efficient manner to regulate the system frequency in coordination with the reheat turbine system and EVs, respectively. Also, the optimization of the parameters for these controllers is another important issue that had to be considered.

The dynamic model of isolated MG with proposed adaptive droop control (ADC) and fuzzy PI is illustrated in Fig. 4. The adaptive droop control mechanism which controls the charging and discharging of EVs is discussed in detail in the following section. Moreover, the fuzzy-PI controller, which is implemented to manage the RTS output according to the system Δf, is also discussed thoroughly in the next section. The optimization for the fuzzy-PI controller parameters is performed by an advanced GA to find the optimal solution.

B. ADAPTIVE DROOP CONTROL AND FUZZY PI CONTROLLERS

In this section, the ADC and fuzzy PI control mechanisms are implemented on EVs and RTS, respectively.

1) ADAPTIVE DROOP CONTROL

The advanced version of conventional droop is ADC, which is widely used in literature for stabilizing an electric power system. The ADC receives information about the frequency

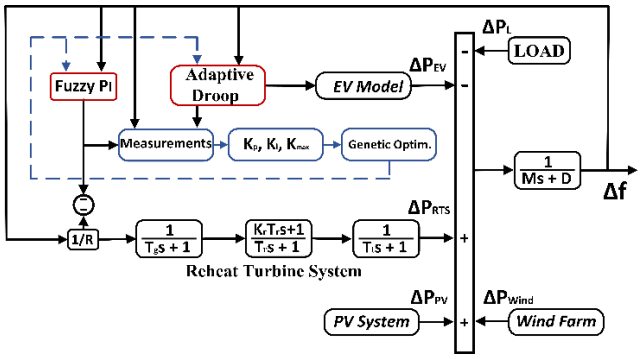

FIGURE 5. Isolated microgrid with the proposed ADC and Fuzzy PI controllers.

variations, the initial state of charge (SOC_i^{in}) and the current state of charge of EVs battery is given in Fig. 3. After checking the power situation at MG, it gives a signal to the EV battery, either to charge or to regulate their SOC. The EV battery charging current (I_{ch_i}) has three inputs, which are initial soc (SOC^{in}), Δf and total plugin time (t_p) as given in Eq. (8). I_{ch_dis} varies according to the Δf, furthermore this current charge the battery by stimulating the EV voltage (V_{soc}). Here the battery system will look into the lookup table and increase/decrease the voltage according to the requirements of MG.

$$I_{ch\_i} = \left(\frac{SOC_i^{max} - SOC_i^{in}}{t_i^p}\right) C_{EV} \tag{8}$$

All the parameters in the above equation are known except the SOC_i^{in}. It is the charge(power) remaining in the EV battery, calculated as the ratio of the EV's distance covered range (d) to maximum distance covered range (dm), which is described as follows:

$$SOC_i^{in} = \left(1 - \frac{d}{dm}\right) \times 100 \tag{9}$$

The daily distance covered range is defined as the long normal distribution by [43]:

$$F_d = \frac{1}{\sqrt[d]{2\pi\sigma^2}} e^{-\frac{(\ln d - \mu)^2}{2\sigma^2}}, \quad d > 0 \tag{10}$$

where $\mu = 3.2$ and $\sigma = 0.9$.

The overall operation of ADC is explained in the flow chart in Fig. 6, where the lower and upper limits of frequency deviation are defined by Δf^L and Δf^U, respectively. To avoid the frequent switching between charging and discharging the dead band is added, here the batteries perform their normal function. Previously the researchers didn't consider these limits [36]c, however, in [42] the researchers consider these limits but didn't consider the integration of RESs. In this work, ADC is used as the first line of defense to respond to the frequency variations. Hence, the ADC is responsible to charge and discharge the EVs according to the information received from the mismatch between the power generations and loads of the proposed system.

The frequency deviations of the system face two abnormal situations either the Δf is greater than Δf^U or Δf less than Δf^L. The first case depicts power generation is greater than power consumption, therefore the EVs charging mode is activated. Now, a priority-based charging of the EVs takes place, all the EVs whose SOC is less than SOC^d are charged first to the desired level by generating the droop based on eq (11). Hereafter the frequency deviation still prevails, so the EVs are charged to SOC^{max} by droop Eq. (12). Meanwhile, the EVs, which are charged to SOC^{max} are disconnected and keep them available for discharging when Δf is less than Δf^L. Additionally, if the frequency deviation is still above the upper limit the ADC simultaneously sends signals to the fuzzy PI to reduce the RTS speed to bring back the frequency to a nominal value.

In the second scenario when the deviation of the system frequency is less than the lower limits i-e Δf is less than Δf^L. Here all the EVs whose SOC is greater than or equal to SOC^d are set to discharge as in Eq. (13). Hence it provides two folded benefits, the first is to preserve enough power for the EVs owner for future usage (driving) and secondly to prolong the EV's battery lifetime [44]. All the EVs, whose SOC is less than SOC^{max}, are set to charging. The following equations (11-13) are related to the flow chart.

$$K_{i,t}^{ch} = \frac{1}{2} K_{i,max} \left(1 + \left[\frac{SOC_i^{in} - SOC^d}{SOC^{min} - SOC^d}\right]^{0.5}\right) \tag{11}$$

$$K_{i,t}^{ch} = \frac{1}{2} K_{i,max} \left(1 + \left[\frac{SOC_i^{in} - SOC^d}{SOC^d - SOC^{max}}\right]^{0.5}\right) \tag{12}$$

$$K_{i,t}^{dis} = \frac{1}{2} K_{i,max} \left(1 + \left[\frac{SOC_i^{in} - SOC^d}{SOC^{max} - SOC^d}\right]^{0.5}\right) \tag{13}$$

2) FUZZY PI CONTROLLER

To investigate the frequency control based on the optimal values of the fuzzy controller parameters, the Genetic Algorithm Optimization Toolbox (GAOT) algorithm is used [45]. Fuzzy, adaptive, and allied controllers are vastly investigated for various control purposes in industries and power systems [46]–[50]. To find the desired frequency regulation performance of the MG integrated with RES, prosumers, and non-RES, a GAOT-based fuzzy logic control design is proposed. The variations in the frequency caused due to the unpredictable nature of the RES and loads are minimized to the acceptable range by applying this technique. For this purpose, the proper gain values are multiplied to the inputs and output to bring them to a suitable range. The Δf and rate of change of frequency deviation ($d\Delta f$) are taken as the inputs and the provided control signal is considered to change the operating point of the entities participating in frequency regulation.

The overall fuzzy logic PI (FLPI) control diagram is presented in Fig. 7. Here the 1/S represents the integrator of

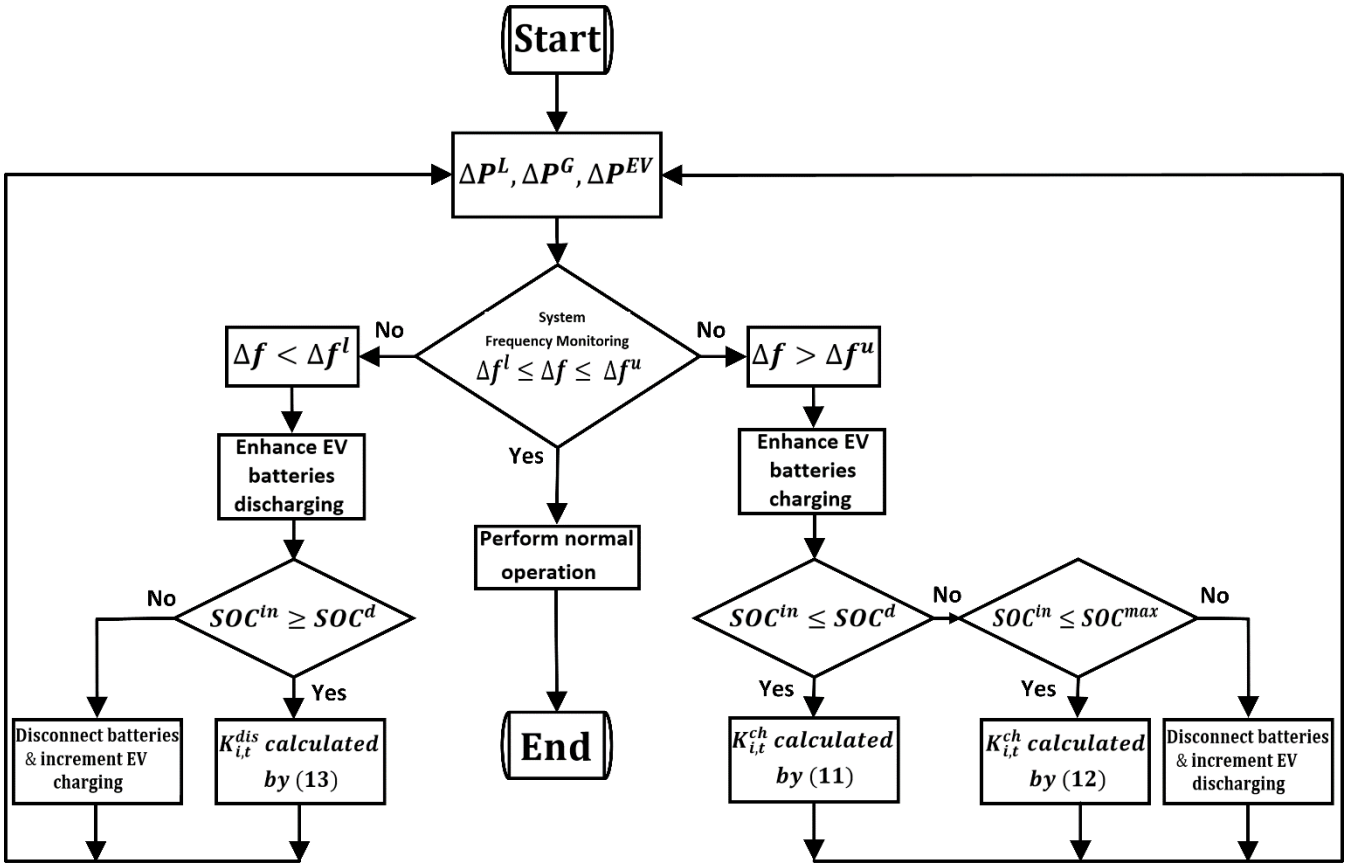

FIGURE 6. Flow chart of ADC.

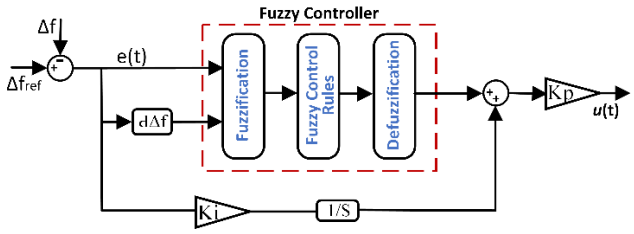

FIGURE 7. Fuzzy controller block diagram.

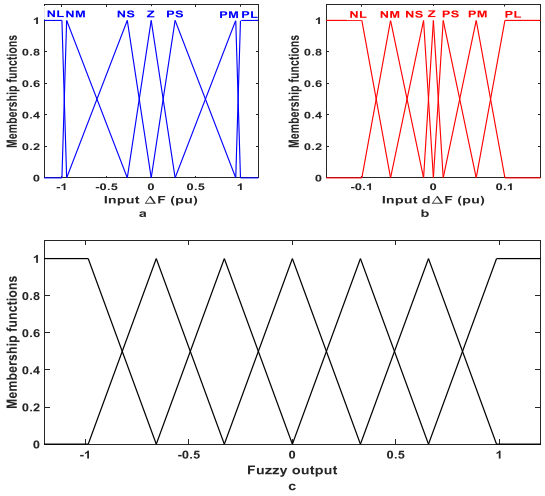

FIGURE 8. (a) Symmetric fuzzy member function Δf. (b) Symmetric fuzzy member function $d\Delta f$. (c) Fuzzy output pattern.

the fuzzy PI controller. Also, e(t) represents the error signal between the reference frequency and the measured frequency. In Fig. 8, the Mamdani-type inference system is presented where the inputs are shown by 7 triangular membership functions as depicted in Fig. 8(a)-(b) and output variables in Fig. 8(c) [34].

The membership functions are described as large negative (LN), large positive (LP), medium negative (MN), medium positive (MP), small negative (SN), small positive (SP), and zero (Z). The mathematical description of the membership functions is defined in Eq. (14), the triangular shape of the membership function is to achieve the controller quick response.

$$\mu_X(x_i) = \max\left(0, 1 - \left|\frac{x - x_i}{c}\right|\right) \tag{14}$$

where x_i and x are the crisp variable, mean of the fuzzy set μ_X, respectively. "Max" represents the maximum value of

TABLE 1. Fuzzy rule base.

Δf \ $d\Delta f$	NL	NM	NS	Z	PS	PM	PL
NL	PL	PL	PL	PM	PM	PS	Z
NM	PL	PM	PM	PM	PS	Z	NS
NS	PL	PM	PS	PS	Z	NS	MN
Z	PM	PM	PS	Z	NS	NM	MN
PS	PM	PS	Z	NS	NS	NM	NL
PM	PS	Z	NS	NM	NM	NM	NL
PL	Z	NS	NM	NM	NL	NL	NL

TABLE 2. Genetic algorithm parameters.

Parameters	Value	Parameters	Value
Number of Variables	3	Populations	50
Variables	K_p, K_i, K_{max}	Iterations	50
Lower Bounds	[−100 −100 0.001]	Crossover	$S_{\text{ingle Point}}$
Upper Bounds	[100 100 10]	Mutation	80%

the two entities given in the equation. c is the spread of the fuzzy set μ_X.

To plot the input space into the output space a logical operation based upon the fuzzy rule base is required. In this paper, the 49 rules base is considered as given in Table 2, the Δf and $d\Delta f$ are the two input vectors on which the rule base is based to perform its operation. The fuzzy rules rely on IF-THEN condition by using Table 1 as follows:

IF Δf is SN **AND** $d\Delta f$ is MP, **THEN** output is SN.

The **IF** condition comprised of two inputs having "AND" an algebraic product operator. By taking into account (14), the former part of this statement can be defined as in (15):

$$\mu_{(\Delta f \text{ AND } d\Delta f)}(x, y) = \mu_{(\Delta f)}(x) . \mu_{(d\Delta f)}(y) \tag{15}$$

where the $\mu_{(\Delta f AND d\Delta f)}$ is the membership value of the linguistic variables, which is the basic entity that defines the fuzzy rules. Hence, the fuzzification process is utilized to map the crisp inputs to linguistic value. Meanwhile, the summation technique is used to combine all the rules to yield the decision value. Lastly, the centroid approach is employed for defuzzification of output fuzzy values to retrieve the crisp values [34].

Since the membership functions are directly associated with the performance of the fuzzy system and to attain good performance results from the controller, a GAOT algorithm is used. This novel GAOT algorithm accurate tuning and find the best optimal values for the parameters of membership functions (MFs). In Fig. 7, the a and b are the set of input MFs respectively, where their range is defined as min $<$ a $<$ b $<$ max. Likewise, one parameter for control output is required to be defined. Consequently, the GAOT algorithm is used to optimize the two parameters of the fuzzy PI (k_p, k_i) for the RTS and the ADC parameter (k_{max}) for the EV. The

TABLE 3. System parameters.

Parameters	Value	Parameters	Value
RTS reheater gain K_r	1/6	WTS inertia constant M_w (s)	5
RTS reheater time Constant T_r (s)	12	WTS time constant T_w (s)	0.2
RTS governor time Constant T_g (s)	0.2	WTS K_{iw} parameter	2.3
RTS turbine time Constant T_t (s)	2	WTS K_{pw} parameter	4.7
Inertia constant M (s)	8.8	EV gain K_{ev}	1
Load damping Constant D	1	EV battery time constant T_{ev}(s)	1
Droop coefficient R	0.05	SOC^{min}	0.2
Dead Band (p.u)	0.001	SOC^{max}	0.95
Battery Capacity of EVs (kWh)	16	SOC^{d}	0.6

optimization purpose is to find the parameters of the fuzzy PI of the RTS and the parameter of the ADC of the EV. The main purpose of the cost function in Eq. (16) is to get optimal parameters that give the optimal frequency performance with less control effort of the RTS and EV. Therefore the cost function purpose is minimizing the sum of these variables $((U_{FLPI})^2$ for the RTS, $(U_{ADC})^2$ for the EV, and $|\Delta f|$ for the frequency regulation. The parameters of the GAOT algorithm are given in Table 2.

$$J = \min(0.001 * \left((U_{FLPI})^2 + (U_{ADC})^2\right) + 0.999 * (|\Delta f|)) \tag{16}$$

Remark 1. The control effort of the proposed fuzzy PI and adaptive droop controllers are changing suddenly, which is not applicable in some other applications such as industrial and robot applications.

IV. SIMULATION RESULTS AND DISCUSSIONS

The isolated MG is modeled in MATLAB/Simulink (R2016a), the system parameters of the isolated microgrid (MG) are given in Table 3. Meanwhile, 49 fuzzy rules are utilized to operate the fuzzy PI controller. The GA algorithm is used to get the optimal values for the adaptive droop control (ADC) and fuzzy PI parameters. The optimal values for fuzzy PI parameters from GA are calculated as, $k_p = -1.5746$ and $k_i = -5.2011$ and the ADC parameter is $k_{max} = 1.5011$. For comparisons purposes, a PI controller is used. This PI controller is well-tuned using the GA with the same options. The resultant parameters for the PI controller are $k_p = 9.1$ and $k_i = 7.7$.

A. CASE 1: MULTI-STEP OF LOAD CHANGE WITH THE REHEAT TURBINE SYSTEM

The performance of the fuzzy PI controller implemented on RTS under the multi-step load variation (ΔP_L) is displayed in Fig. 9 (a). The main reason behind the consideration of

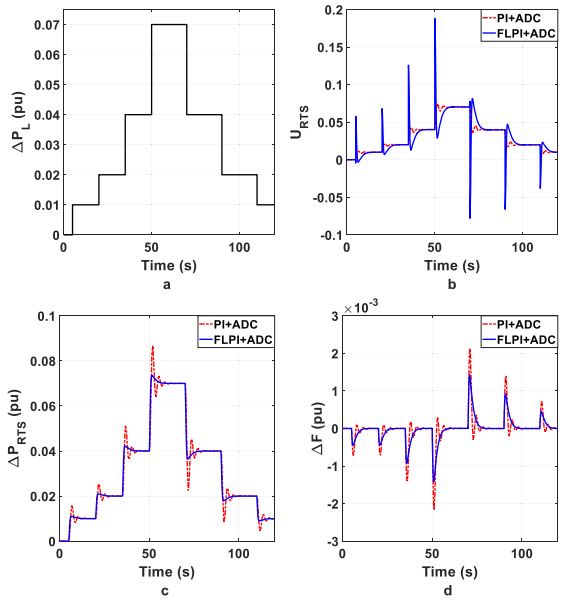

FIGURE 9. The PI and Fuzzy PI controllers' results (a) ΔP_L (b) U_{RTS} (c) ΔP_{RTS} (d) Δf.

RTS is to validate the performance of the fuzzy PI controller and to make a comparison between the PI and the fuzzy PI controller.

In Fig. 9 (b), the U_{RTS} represents the input signal fed to the RTS by these controllers. The output power from RTS (ΔP_{RTS}) is displayed in Fig. 9 (c). The frequency change (Δf) of the isolated MG according to load variations and by using the PI and fuzzy PI controller is presented in Fig. 9 (d). From Fig. 9(a), the step load gradually increased from 0.01 to 0.07pu at time ($t = 0s$ *to* $t = 50s$), and gradually decreased from 0.07 to 0.01pu at time ($t = 65s$ *to* $t = 110s$). During the overall load change, the fuzzy PI controller shows significantly better frequency performance in minimizing the overshoot and settling time in comparison with the PI controller. Besides, it is evident that both controllers restore the system frequency to the nominal limits.

B. CASE 2: MULTI-STEP OF LOAD CHANGE WITH THE REHEAT TURBINE SYSTEM AND EVs

In the second case, the EVs (ΔP_{EV}) integration effect is studied by considering the same load variation (ΔP_L) and the RTS. From Fig. 10(a), the load gradually increases from 0.01 to 0.02pu at a time (t = 0s to t = 20s), and a huge increase at a time (t = 35s and t = 50s) is observed. In the specified time intervals, the fuzzy PI and adaptive droop control (FLPI-PI) controller well managed the charging of EVs batteries, to attain their desired state of charge (SOC) level as shown in Fig. 10(h). For a gradual decrease in load from 0.02 to 0.01pu at a time (t = 85s to t = 110s) and for a huge load change from 0.07 to 0.02pu at a time (t = 65s to t = 85s), the FLPI-ADC controllers show almost the same frequency performance in comparison with the PI and adaptive droop control (PI-ADC) controllers.

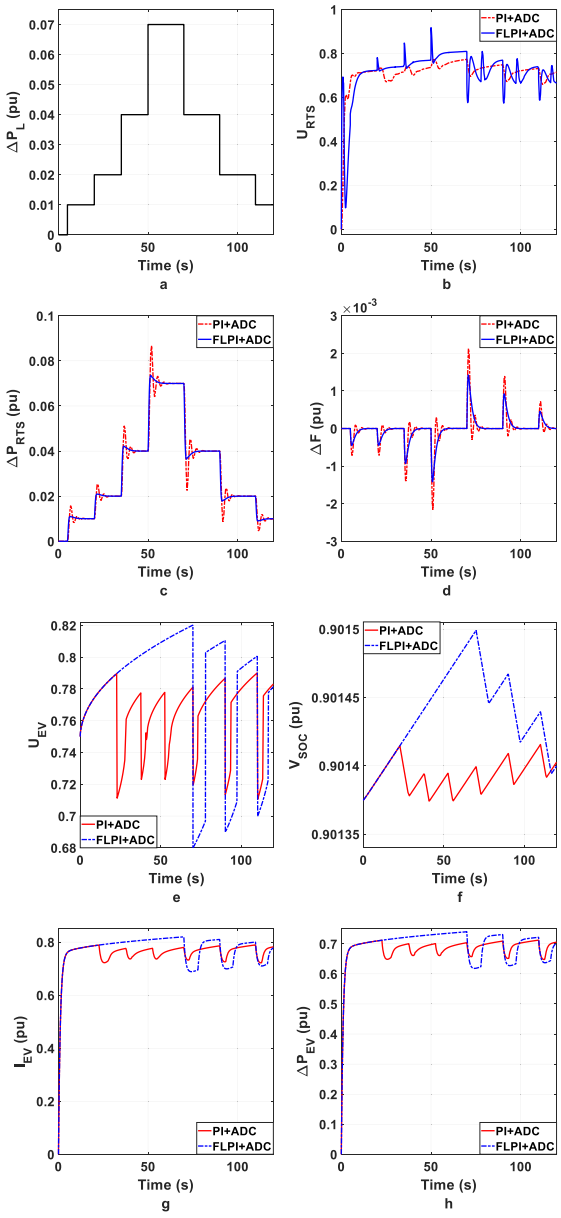

FIGURE 10. The PI and Fuzzy PI controllers results (a) ΔP_L (b) U_{RTS} (c) ΔP_{RTS} (d) Δf (e) U_{EV} (f) V_{EV} (g) I_{EV} (h) ΔP_{EV}.

The performance of FLPI-ADC controllers seems as not good as of the PI-ADC controllers at time $t = 65s$. The FLPI-ADC controllers discharge the EVs batteries to help the RTS for managing the ΔP_L, meanwhile, the ΔP_L is also reduced from 0.07 to 0.04pu. This causes more generation than the load results in a positive Δf at this moment. Moreover, at $t = 85s$ the SOC of the EVs batteries are less than their desired level, so the FLPI-ADC controllers first charge the EVs batteries to manages their desired SOC. Thus, at this instant, the EVs draw power from the MG instead of providing power resulting in deviation in system frequency. Conversely, the PI-ADC controllers only charge and discharge the EVs but didn't properly consider the EVs provision in

providing power support to the RTS in the frequency regulation. In Fig.10 (e), the U_{EV} represents the input signal fed to the EVs by the controllers to regulate the ΔP_{EV} (Fig.10(h)), the FLPI-ADC controllers show better performance in managing the voltage (V_{EV}), current (I_{EV}) of the EVs batteries, and their interaction with the load demand (ΔP_{EV}) than the PI-ADC controllers. Furthermore, the former controllers provide better performance than the latter controllers in system frequency regulation (Δf) in minimizing the overshoot and settling time as displayed in Fig. 10(d).

C. CASE 3: MULTI-STEP OF LOAD CHANGE WITH THE REHEAT TURBINE SYSTEM, EVS, AND RENEWABLE ENERGY SOURCES

In this case, the effect of the WTS output power and PV output power are investigated, to support the RTS in fulfilling the load demand (ΔP_L) besides the EVs. The U_{EV} (Fig.11 (e)) represents the input signal fed to the EV by the FLPI-ADC controllers and, PI-ADC controllers. The FLPI-ADC controllers manage the voltage (V_{EV}), current (I_{EV}) and power of the EVs batteries in a better and efficient manner by fulfilling the energy demands of the EVs and respond accordingly to the system frequency than the PI- ADC controllers, as shown in Fig. 11 (f), Fig. 11 (g) and Fig. 11 (h), respectively.

Initially, from time ($t = 0s\ to\ t = 65s$), the WTS produces a constant power (ΔP_W) of 0.035pu and PV power generation (ΔP_{PV}) shows a slight decrease from 0.13 to 0.1pu at the wind speed and solar irradiation is displayed in Fig. 11(j) and Fig. 11(i), respectively. At time $t = 65s$, the reduction in ΔP_{PV} is well sensed by the FLPI-ADC controllers, so the EVs discharge their batteries to support the RTS. Meanwhile, at this instant the ΔP_L is also reduced, consequently, the system possesses extra power generation than the load demand, results in a positive Δf (Fig. 11(d)).

The Δf appeared at this moment is still in its nominal limits and in fact, it validates the better performance of the FLPI-ADC control mechanism to regulate the ΔP_{EV} according to the system requirement.

However, the PI-ADC controllers have not properly charge and discharge the EVs according to the load situations and put all the burden of power regulation on RTS (Fig. 11(c)). During the overall load change, the FLPI-ADC controllers show significantly better frequency performance in minimizing the overshoot and settling time in comparison with the PI-ADC controllers.

D. CASE 4: VARIABLE LOAD CHANGE WITH THE REHEAT TURBINE SYSTEM, EVS, AND VARIABLE RENEWABLE ENERGY SOURCES

In this case, the MG frequency performance is examined while considering a variable load (ΔP_L) instead of a multistep load disturbance (Fig. 12(a)), to demonstrate the performance and efficiency of the proposed controllers. The effect of variable wind speed which varies between 9 and 12 meters per seconds, and the variable irradiance (Fig. 12(i)), on the WTS output power generation and PV output power generation (Fig.12(j)), are considered along with the RTS and EVs. The input signal (U_{RTS}) generated to regulate the power of RTS (ΔP_{RTS}) is displayed in Fig. 12(b).

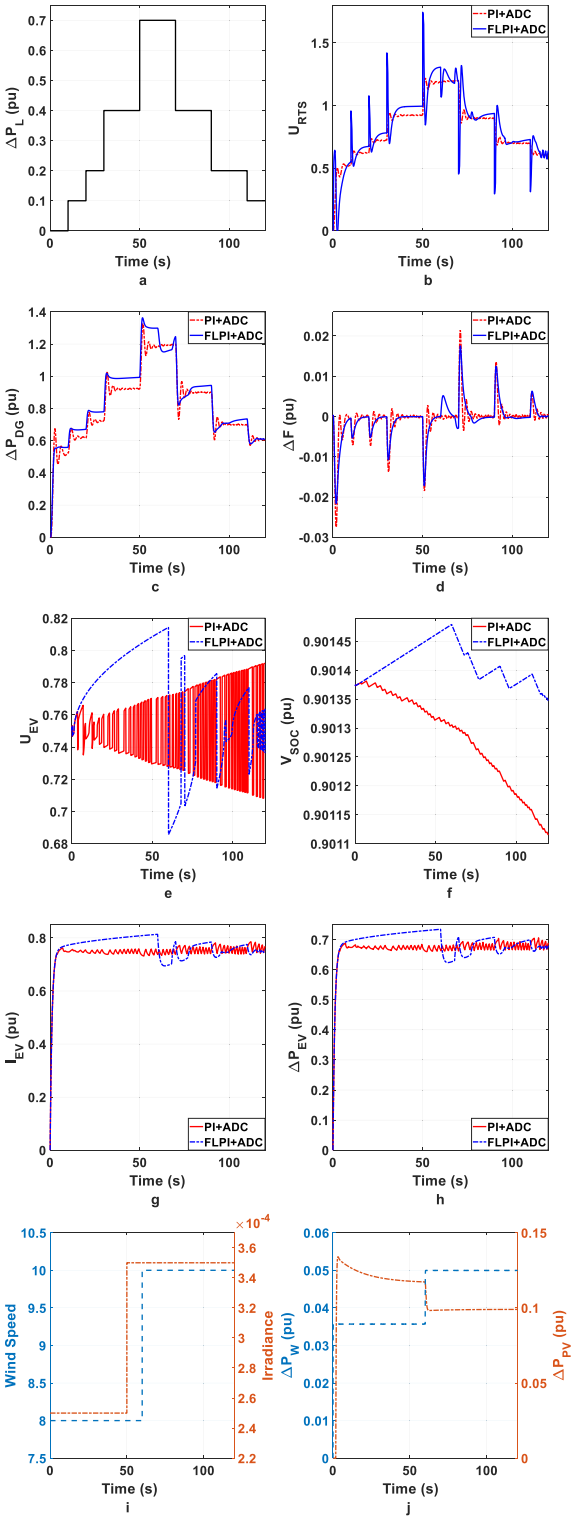

FIGURE 11. The PI and Fuzzy PI controllers results (a) ΔP_L (b) U_{RTS} (c) ΔP_{RTS} (d) Δf (e) U_{EV} (f) V_{EV} (g) I_{EV} (h) ΔP_{EV} (i) wind speed and irradiation (j) ΔP_W and ΔP_{PV}.

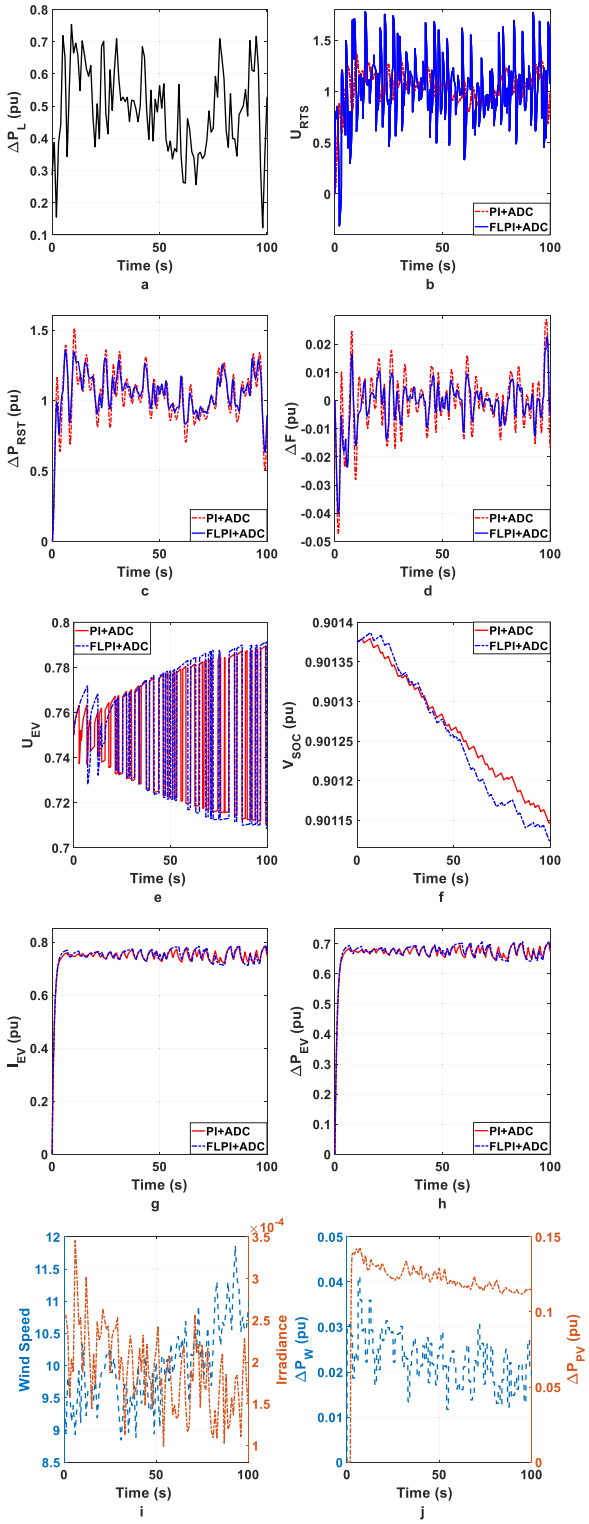

FIGURE 12. The PI and Fuzzy PI controllers results (a) ΔP_L (b) U_{RTS} (c) ΔP_{RTS} (d) Δf (e) U_{EV} (f) V_{EV} (g) I_{EV} (h) ΔP_{EV} (i) wind speed and irradiation (j) ΔP_W and ΔP_{PV}.

Here, additional power is added to the system by RESs, therefore, the power share from the RTS is reduced. The change in the frequency (Δf) of isolated MG according to ΔP_L and by using the FLPI-ADC and PI-ADC controllers are presented in Fig. 12(d). In Fig.12(e), the U_{EV} represents the input signal feed to the EV by the ADC. The voltage (V_{EV}) and current (I_{EV}) of the EV battery are displayed in Fig. 12(f) and Fig. 12(g), respectively. The output power (ΔP_{EV}) from EV is displayed in Fig. 12(h).

During the variable load change, the FLPI-ADC controllers show a significantly better frequency performance in minimizing the overshoot and settling time in comparison with the PI controller. From the above discussion, it is obvious that both controllers restore the system frequency to the nominal limits. Also, the FLPI-ADC controllers regulate the ΔP_{EV} according to the frequency deviation in order to participate effectively in frequency regulation of the isolated MG and its performance is better than the PI-ADC controller.

V. CONCLUSION

This paper presents an isolated MG to study the impact of fuzzy PI and adaptive droop control to regulate the system frequency within the desirable limits. Here, the reheat turbine system provides the main chunk of power. Meanwhile, to utilize the maximum output power, the RESs are not controlled. The intermittency of the RESs cause power variations and hence yield frequency deviations. To counter these effects EVs are included in the MG environment. As the EVs contain batteries that have the charging and discharging capabilities therefore, they are a good reciprocal of the energy storage system. The EVs are maintained to the desired SOC limits to have power for the driving needs as well. Four case studies are presented here, in the first case, the RTS system is studied alone and in the second case, the EVs are added. The impact of PI, ADC, and fuzzy PI, ADC is analyzed, the latter shows the best performance results. In the third and fourth cases, the constant and variable RESs are integrated into the isolated MG. The same two combinations of controllers are applied to check the system performance. The fuzzy PI and ADC provide better performance results in the stabilization of the system frequency.

In the future, an advanced model predictive control technique and adaptive droop control combination will be applied to an isolated MG for frequency regulation. Moreover, an additional energy storage system will be added to study the effect of the energy storage besides the EVs on the MG system.

REFERENCES

[1] R. H. Lasseter and P. Paigi, "Microgrid: A conceptual solution," in *Proc. IEEE 35th Annu. Power Electron. Spec. Conf.*, Jun. 2004, pp. 4285–4290.

[2] H. Bevrani, A. Ghosh, and G. Ledwich, "Renewable energy sources and frequency regulation: Survey and new perspectives," *IET Renew. Power Gener.*, vol. 4, no. 5, p. 438, Sep. 2010.

[3] S. Iqbal, A. Xin, M. U. Jan, S. Salman, A. U. M. Zaki, H. U. Rehman, M. F. Shinwari, and M. A. Abdelbaky, "V2G strategy for primary frequency control of an industrial microgrid considering the charging station operator," *Electronics*, vol. 9, no. 4, p. 549, 2020.

[4] J. I. Leon, S. Vazquez, and L. G. Franquelo, "Multilevel converters: Control and modulation techniques for their operation and industrial applications," *Proc. IEEE*, vol. 105, no. 11, pp. 2066–2081, Nov. 2017.

[5] L. A. de Souza Ribeiro, O. R. Saavedra, S. L. de Lima, and J. G. de Matos, "Isolated micro-grids with renewable hybrid generation: The case of Lençóis island," *IEEE Trans. Sustain. Energy*, vol. 2, no. 1, pp. 1–11, Jan. 2011.

[6] H. Bevrani, M. R. Feizi, and S. Ataee, "Robust frequency control in an islanded microgrid: H_∞ and μ-Synthesis approaches," *IEEE Trans. Smart Grid*, vol. 7, no. 2, pp. 706–717, Mar. 2015.

[7] S. Vazquez, S. Lukic, E. Galvan, L. G. Franquelo, J. M. Carrasco, and J. I. Leon, "Recent advances on energy storage systems," in *Proc. IECON 37th Annu. Conf. IEEE Ind. Electron. Soc.*, Nov. 2011, pp. 4636–4640.

[8] M. Lotfy, T. Senjyu, M. Farahat, A. Abdel-Gawad, and A. Yona, "A frequency control approach for hybrid power system using multi-objective optimization," *Energies*, vol. 10, no. 1, p. 80, 2017.

[9] X. Tan, Q. Li, and H. Wang, "Advances and trends of energy storage technology in microgrid," *Int. J. Electr. Power Energy Syst.*, vol. 44, no. 1, pp. 179–191, Jan. 2013.

[10] D. Xu, J. Liu, X.-G. Yan, and W. Yan, "A novel adaptive neural network constrained control for a multi-area interconnected power system with hybrid energy storage," *IEEE Trans. Ind. Electron.*, vol. 65, no. 8, pp. 6625–6634, Aug. 2018.

[11] W. Kempton and S. E. Letendre, "Electric vehicles as a new power source for electric utilities," *Transp. Res. D, Transp. Environ.*, vol. 2, no. 3, pp. 157–175, Sep. 1997.

[12] H. Han, X. Hou, J. Yang, J. Wu, M. Su, and J. M. Guerrero, "Review of power sharing control strategies for islanding operation of AC microgrids," *IEEE Trans. Smart Grid*, vol. 7, no. 1, pp. 200–215, Jan. 2016.

[13] P. Wu, W. Huang, N. Tai, Z. Ma, X. Zheng, and Y. Zhang, "A multi-layer coordinated control scheme to improve the operation friendliness of grid-connected multiple microgrids," *Energies*, vol. 12, no. 2, p. 255, 2019.

[14] Q. Sun, Q. Sun, and D. Qin, "Adaptive fuzzy droop control for optimized power sharing in an islanded microgrid," *Energies*, vol. 12, no. 1, p. 45, 2018.

[15] X.-H. Chang, Y. Liu, and M. Shen, "Resilient control design for lateral motion regulation of intelligent vehicle," *IEEE/ASME Trans. Mechatronics*, vol. 24, no. 6, pp. 2488–2497, Dec. 2019.

[16] J. Liu, H. An, Y. Gao, C. Wang, and L. Wu, "Adaptive control of hypersonic flight vehicles with limited angle-of-attack," *IEEE/ASME Trans. Mechatronics*, vol. 23, no. 2, pp. 883–894, Apr. 2018.

[17] M. Datta and T. Senjyu, "Fuzzy control of distributed PV inverters/energy storage systems/electric vehicles for frequency regulation in a large power system," *IEEE Trans. Smart Grid*, vol. 4, no. 1, pp. 479–488, Mar. 2013.

[18] K. De Craemer, S. Vandael, B. Claessens, and G. Deconinck, "An event-driven dual coordination mechanism for demand side management of PHEVs," *IEEE Trans. Smart Grid*, vol. 5, no. 2, pp. 751–760, Mar. 2014.

[19] M. Aziz, T. Oda, T. Mitani, Y. Watanabe, and T. Kashiwagi, "Utilization of electric vehicles and their used batteries for peak-load shifting," *Energies*, vol. 8, no. 5, pp. 3720–3738, 2015.

[20] I. Pavić, T. Capuder, and I. Kuzle, "Value of flexible electric vehicles in providing spinning reserve services," *Appl. Energy*, vol. 157, pp. 60–74, Nov. 2015.

[21] K. M. Rogers, R. Klump, H. Khurana, A. A. Aquino-Lugo, and T. J. Overbye, "An authenticated control framework for distributed voltage support on the smart grid," *IEEE Trans. Smart Grid*, vol. 1, no. 1, pp. 40–47, Jun. 2010.

[22] H. Fan, L. Jiang, C.-K. Zhang, and C. Mao, "Frequency regulation of multi-area power systems with plug-in electric vehicles considering communication delays," *IET Gener., Transmiss. Distrib.*, vol. 10, no. 14, pp. 3481–3491, Nov. 2016.

[23] J. M. Guerrero, J. C. Vasquez, and R. Teodorescu, "Hierarchical control of droop-controlled DC and AC microgrids—A general approach towards standardization," in *Proc. 35th Annu. Conf. IEEE Ind. Electron.*, vol. 58, no. 1, pp. 158–172, Jan. 2011.

[24] D. H. Tungadio and R. C. Bansal, "Active power reserve estimation of two interconnected microgrids," *Energy Procedia*, vol. 105, pp. 3909–3914, May 2017.

[25] N. Nikmehr and S. Najafi Ravadanegh, "Reliability evaluation of multi-microgrids considering optimal operation of small scale energy zones under load-generation uncertainties," *Int. J. Electr. Power Energy Syst.*, vol. 78, pp. 80–87, Jun. 2016.

[26] Y. Xu, C. Li, Z. Wang, N. Zhang, and B. Peng, "Load frequency control of a novel renewable energy integrated micro-grid containing pumped hydropower energy storage," *IEEE Access*, vol. 6, pp. 29067–29077, 2018.

[27] D. H. Tungadio, R. C. Bansal, M. W. Siti, and N. T. Mbungu, "Predictive active power control of two interconnected microgrids," *Technol. Econ. Smart Grids Sustain. Energy*, vol. 3, no. 1, p. 3, Dec. 2018.

[28] C. Peng and J. Zhang, "Delay-distribution-dependent load frequency control of power systems with probabilistic interval delays," *IEEE Trans. Power Syst.*, vol. 31, no. 4, pp. 3309–3317, Jul. 2016.

[29] M. N. Anwar and S. Pan, "A new PID load frequency controller design method in frequency domain through direct synthesis approach," *Int. J. Electr. Power Energy Syst.*, vol. 67, pp. 560–569, May 2015.

[30] M. A. K. El-Shafei, M. I. El-Hawwary, and H. M. Emara, "Implementation of fractional-order PID controller in an industrial distributed control system," in *Proc. 14th Int. Multi-Conf. Syst., Signals Devices (SSD)*, Mar. 2017, pp. 713–718.

[31] A. Annamraju and S. Nandiraju, "Robust frequency control in a renewable penetrated power system: An adaptive fractional order-fuzzy approach," *Protection Control Modern Power Syst.*, vol. 4, no. 1, p. 16, Dec. 2019.

[32] X. Liu, Y. Zhang, and K. Y. Lee, "Coordinated distributed MPC for load frequency control of power system with wind farms," *IEEE Trans. Ind. Electron.*, vol. 64, no. 6, pp. 5140–5150, Jun. 2017.

[33] X. Kong, X. Liu, L. Ma, and K. Y. Lee, "Hierarchical distributed model predictive control of standalone Wind/Solar/Battery power system," *IEEE Trans. Syst., Man, Cybern. Syst.*, vol. 49, no. 8, pp. 1570–1581, Aug. 2019.

[34] H. Bevrani and P. R. Daneshmand, "Fuzzy logic-based load-frequency control concerning high penetration of wind turbines," *IEEE Syst. J.*, vol. 6, no. 1, pp. 173–180, Mar. 2012.

[35] J. R. Pillai and B. Bak-Jensen, "Integration of vehicle-to-grid in the western danish power system," *IEEE Trans. Sustain. Energy*, vol. 2, no. 1, pp. 12–19, Jan. 2011.

[36] M. A. Abdelbaky, X. Liu, and D. Jiang, "Design and implementation of partial offline fuzzy model-predictive pitch controller for large-scale wind-turbines," *Renew. Energy*, vol. 145, pp. 981–996, Jan. 2020.

[37] M. A. Abdelbaky, X. Liu, and X. Kong, "Wind turbines pitch controller using constrained fuzzy-receding horizon control," in *Proc. Chin. Control Decis. Conf. (CCDC)*, Jun. 2019, pp. 236–241.

[38] M. Jalali and K. Bhattacharya, "Frequency regulation and AGC in isolated systems with DFIG-based wind turbines," in *Proc. IEEE Power Energy Soc. Gen. Meeting*, Jul. 2013, pp. 1–5.

[39] X. Kong, L. Ma, X. Liu, M. A. Abdelbaky, and Q. Wu, "Wind turbine control using nonlinear economic model predictive control over all operating regions," *Energies*, vol. 13, no. 1, p. 184, 2020.

[40] D.-J. Lee and L. Wang, "Small-signal stability analysis of an autonomous hybrid renewable energy power generation/energy storage system—Part I: Time-domain simulations," *IEEE Trans. Energy Convers.*, vol. 23, no. 1, pp. 311–320, Mar. 2008.

[41] E. K. Belal, D. M. Yehia, and A. M. Azmy, "Adaptive droop control for balancing SOC of distributed batteries in DC microgrids," *IET Gener., Transmiss. Distrib.*, vol. 13, no. 20, pp. 4667–4676, Oct. 2019.

[42] H. Jia, X. Li, Y. Mu, C. Xu, Y. Jiang, X. Yu, J. Wu, and C. Dong, "Coordinated control for EV aggregators and power plants in frequency regulation considering time-varying delays," *Appl. Energy*, vol. 210, pp. 1363–1376, Jan. 2018.

[43] J. Tan and L. Wang, "Assessing the impact of PHEVs on load frequency control with high penetration of wind power," in *Proc. IEEE PES T&D Conf. Expo.*, Apr. 2014, pp. 1–5.

[44] (2010). *Modelling Electric Storage Devices for Electric Vehicles*. Accessed: Feb. 28, 2019. [Online]. Available: http://www.ev-merge.eu/images/stories/uploads/ MERGE_WP2_D2.1.pdf

[45] M. Patrascu and A. Ion, "Evolutionary modeling of industrial plants and design of PID controllers," in *Nature-Inspired Computing for Control Systems*. Cham, Switzerland: Springer, 2016, pp. 73–119.

[46] X.-H. Chang and G.-H. Yang, "Nonfragile H_∞ filtering of continuous-time fuzzy systems," *IEEE Trans. Signal Process.*, vol. 59, no. 4, pp. 1528–1538, Apr. 2011.

[47] X.-H. Chang, *Takagi-Sugeno Fuzzy Systems Non-Fragile H-Infinity Filtering*, vol. 282. Cham, Switzerland: Springer, 2012.

[48] Y. Zhao, J. Wang, F. Yan, and Y. Shen, "Adaptive sliding mode fault-tolerant control for type-2 fuzzy systems with distributed delays," *Inf. Sci.*, vol. 473, pp. 227–238, Jan. 2019.

[49] C. Wu, J. Liu, X. Jing, H. Li, and L. Wu, "Adaptive fuzzy control for nonlinear networked control systems," *IEEE Trans. Syst., Man, Cybern. Syst.*, vol. 47, no. 8, pp. 2420–2430, Aug. 2017.

[50] G. Sun and Z. Ma, "Practical tracking control of linear motor with adaptive fractional order terminal sliding mode control," *IEEE/ASME Trans. Mechatronics*, vol. 22, no. 6, pp. 2643–2653, Dec. 2017.

MISHKAT ULLAH JAN received the B.Sc. degree in electrical engineering from the University of Engineering and Technology, Bannu, Pakistan, in 2010, and the M.S. degree in electrical engineering from the CECOS University of IT and Emerging Sciences, Peshawar, Pakistan, in 2014. He is currently pursuing the Ph.D. degree in electrical engineering with the North China Electric Power University, Beijing, China.

From 2010 to 2011, he worked as a Trainee Engineer under the National Internship Program at Sarhad Hydel Development Organization, Pakistan. From 2014 to 2015, he worked as a Research Associate with CECOS University, Peshawar, Pakistan. His research interests include power system stability, frequency regulation, and energy management of microgrid.

AI XIN was born in 1964. He received the B.S. degree from the Nanjing Institute of Technology, Nanjing, China (now Southeast University), in 1985, the M.S. degree from the China Electric Power Research Institute, Beijing, China, in 1988, and the Ph.D. degree from North China Electric Power University (NCEPU), Beijing, in 1999, all in electrical engineering. He was a Senior Research Scholar with Brunel University, London, U.K., in 2003. He was the Director of the Institute of Power Systems, NCEPU, where he was engaged in research and teaching on power system and automation. He is currently a Professor and the Ph.D. Tutor with the School of Electrical and Electronic Engineering, NCEPU. His current research interests include power system analysis and control, and transactive energy.

MOHAMED ABDELKARIM ABDELBAKY received the B.Sc. and M.Sc. degrees in electrical engineering from Cairo University, Egypt, in 2013 and 2016, respectively. He is currently pursuing the Ph.D. degree with the School of Control and Computer Engineering, North China Electric Power University, Beijing, China, from 2017.

He has joined the Department of Electrical Power and Machines Engineering, Cairo University, as an Associate Lecturer, in 2016. His current interests include nonlinear and economic model predictive control, their stability analysis, and their applications in wind energy conversion systems, power plants, and power system frequency regulation.

HASEEB UR REHMAN received the B.S. degree in electrical engineering from the University of Engineering and Technology, Bannu, Pakistan, in 2010, and the M.S. degree in electrical engineering from the University of Engineering and Technology, Peshawar, in 2016. He is currently pursuing the Ph.D. degree in electrical engineering with North China Electric Power University, Beijing, China.

From 2012 to 2017, he worked as an Engineer Distribution with Sui Northern Gas Pipeline Ltd, Pakistan. His research interest includes the integration of renewable energy source in microgrid, frequency stability and control of microgrid through virtual synchronous generator.

SHEERAZ IQBAL received the B.E. degree in telecommunication engineering from Allama Iqbal Open University, Islamabad, Pakistan, and the M.S. degree in electronic engineering from the International Islamic University, Islamabad, in 2010 and 2014, respectively. He is currently pursuing the Ph.D. degree in electrical engineering with North China Electric Power University, Beijing, China. He has served as a Lecturer at the Department of Electrical Engineering University of Azad Jammu and Kashmir, Muzaffarabad, Pakistan, from 2014 to 2017. His research interests include primary frequency control, MG energy management, and electric vehicles integration in industrial MG.